Electron transfer dictates metabolic reprogramming in proliferating cells under hypoxia

Yuanyuan Wang,[1,2] † Miao Liu,[2]† Yuxia Ruan,[2] Qiaoyun Chu,[1] Yanfen Cui,[2] Guoguang Ying,[2] and Binghui Li[1,2]*

[1] Department of Biochemistry and Molecular Biology, Capital Medical University, Beijing 100069, P.R. China.

[2]Department of Cancer Cell Biology and National Clinical Research Center for Cancer, Tianjin Medical University Cancer Institute and Hospital, Tianjin 300060, P. R. China.

*Correspondence: bli@ccmu.edu.cn

†Co-first author

Metabolic reprogramming, such as abnormal utilization of glucose, addiction to glutamine and increased *de novo* lipid synthesis, extensively occurs in proliferating cancer cells. This phenomenon occurs highly heterogeneously, but its origin has remained unclear. Here we propose a novel physicochemical concept of *free electron potential* and develop its equation of state to profile metabolites. The free-electron-potential change of substrates and products exactly reflects electrons dissipated or produced in a metabolic transformation. Based on the conservation of electron in chemical reactions, a function of free-electron-potential change for proliferating cells are further derived, and it can accurately predict metabolic behaviors under hypoxia by maximizing its value to consume electrons. Therefore, enabling electron transfer dictates metabolic reprogramming in hypoxic cells, which underlies the major findings in cancer metabolism and is supported by our experiments. Importantly, we reveal a combination of promising targets to inhibit tumor growth under hypoxia by blocking electron transfer.

Life is a self-organizing and self-adaptive system. Therefore, it is not surprising that proliferating cells, such as cancer cells, develop significant metabolic heterogeneity (*1-3*) to cope with the changing microenvironment. As a pool of integrated chemical transformations in cells, metabolism must observe the chemical laws. If we can find out the chemical law underlying metabolic reprogramming in proliferating cancer cells, we may design a cocktail of broad-spectrum treatments for cancers regardless of the heterogeneity. Classically, chemical reactions involve the forming and breaking of chemical bonds between atoms. Since chemical bonds result from a redistribution of the outer electrons of atoms, chemical reactions may encompass electron transfer between each other or release electrons to the system. As for mammalian cells, the established fact is that oxygen is used to accept the net electrons released from the whole cellular metabolism, which is mediated by the mitochondrial electron-transport chain (ETC). Therefore, the mitochondrion plays an essential role as the electron acceptor in enabling cell proliferation in addition to energy generation (*4-6*). However, when the ETC is disabled by hypoxia or pathological/pharmacological inhibition, how to enable electron transfer to support cell proliferation remains elusive. Here, we build up a physicochemical model using a novel concept to reveal the chemical nature of metabolic reprogramming in cells.

Results

Electron transfer in intracellular metabolic reactions

In mammalian cells, the transfer of electrons of compounds to oxygen occurs directly, semi-directly or indirectly by using electron acceptors (Fig. 1A). Direct and semi-direct

oxidations are catalyzed by dioxygenase and monooxygenase, and mainly involved in the catabolism of some compounds with aromatic groups or long aliphatic chains (*7*). In contrast, most of redox transformations are carried out indirectly. The final transfer of indirect electrons to oxygen is coupled to mitochondrial ATP generation (Fig. 1, B and C), which is much more efficient than the other energy-producing pathway, the glycolysis with glucose being converted to lactate (Fig. 1D).

The electron acceptor, FAD/FMN, tightly or covalently binds to its enzymes. After accepting electrons, $FADH_2$/$FMNH_2$ usually immediately transfers electrons to NAD^+ and $NADP^+$, or directly to the ETC (*8*). Therefore, NAD^+ and $NADP^+$ are the major free electron acceptors that link up oxidative and reductive reactions. Electrons in NADH and/or NADPH are compartmentally generated in cells, and they can be easily translocated spatially or transhydrogenated between each other by various biochemical shuttles or reversible biochemical reactions (*9*) (Fig. 1E and fig. S1). Based on the conservation of electron in chemical reactions, the global electrons produced should be equated to those dissipated in a cell, which is indispensable to support cell survival and growth.

Free electron potential of metabolites

To exactly understand the intracellular production and dissipation of global electrons, we invented a physicochemical concept referred to as *free electron potential (FEP)*. *FEP* characterizes the potential ability of a typical biological metabolite, with the molecular formula of $C_CH_HO_ON_N$, to release electrons upon its complete oxidation to CO_2, H_2O and NH_3 in cells. Since oxygen is the electron acceptor, the number of net oxygen atoms required for

complete oxidation represents the electrons released from the metabolite. Based on this concept, we derived an equation of state for *FEP*,

$$Y = 2N_C + (N_H - 3N_N)/2 - N_O \quad (1)$$

in which Y is used as the symbol for *FEP* and N_C, N_H, N_N and N_O are the number of carbon, hydrogen, oxygen and nitrogen atoms in the molecule. Notably, electrons are almost always transferred in pairs in chemical reactions, and one oxygen atom can accept a pair of electrons, thus Y indicates the number of electron pairs. The biological electron acceptors, such as FAD/FMN and $NAD(P)^+$, also accept electrons in pairs and are converted into their reductive forms, $FADH_2$/$FMNH_2$ and NAD(P)H + H^+. Here we listed Y values of intracellular metabolites involved in the metabolism of glucose, amino acids, nucleic acids and lipids (Table 1 and table S1). Interestingly, the Y/C values (Y per carbon atom) of metabolites show somehow internal properties determined by "2" (fig. S2 and section S1.1 and S2.1).

Equation (1) can be used to quantitatively calculate electrons produced in metabolic conversions by *FEP* change, $\Delta Y_{P,S}$, between Y values of initial substrates and those of final products. As for a transformation,

$$S_1 + S_2 + \ldots + S_n \rightarrow P_1 + P_2 + \ldots + P_m,$$

where S and P are the carbon-containing metabolites with the quantity of carbon atoms being made conserved,

$$\Delta Y_{\mathrm{P,S}} = \sum_{j=1}^{m} Y_{\mathrm{P}_j} - \sum_{i=1}^{n} Y_{\mathrm{S}_i} \quad (2)$$

A positive *FEP* change means the consumption of electrons while a negative value indicates the release of electrons in this conversion. Notably, ΔY only depends on initiators and objects independently of detailed metabolic routes (a formal proof detailed in section S1.2). Phosphate group and Co-enzyme are often used to facilitate metabolic transformations, however, their addition to metabolites do not involve the transfer of electrons. Thus we only need to simply focus on the form of compounds without phosphate and Co-enzyme when ΔY is calculated.

Electron transfer in proliferating cells

Mammalian and bacterial cells share the similar chemical compositions (*10*) (table S2). Macromolecules including proteins, nucleic acids, lipids and polysaccharides account for 87% and their precursors involving amino acids, nucleotides, fatty acids, sugars and the related intermediates make up 9.3% of cell mass. The rest chemicals are inorganic ions (3%) that are unrelated to electron transfer and other small molecules (0.7%) that could be negligible to the analysis of global intracellular electrons. Proliferating cells must have active anabolism and ATP generation. Protein synthesis from amino acids, nucleic acid synthesis from nucleosides, polysaccharide synthesis from sugars and lipid synthesis from fatty acids do not involve the transfer of electrons. Therefore, here we only need to focus on the synthesis of amino acids (non-essential amino acids), nucleosides, fatty acids and sugars. The major cellular nutrition

in blood includes glucose and amino acids. Glutamine is the most abundant free amino acid. In addition to the use in protein biosynthesis, glutamine also provides nitrogen source for nucleosides synthesis (*11*) (fig. S3). Like glucose, glutamate, the metabolic product of glutamine after its deamidation in nucleoside synthesis, can also be used as carbon source to synthesize non-essential amino acids and lipids or replenish the citric acid cycle (CAC) (*2*) (fig. S1). We calculated the possible ΔY of these building bricks for cell proliferation based on Y values of metabolites in Table 1 and Extended Data Table 1 (Fig. 2, A-E, and table S3).

To enable intracellular metabolic transformations, electron transfer from oxidations ($\sum\Delta Y_{\text{Metab-}}$) to reductions ($\sum\Delta Y_{\text{Metab+}}$) and the ETC ($\sum\Delta Y_{\text{ETC+}}$) has to keep balanced (Fig. 1C). Therefore, the intracellular net electrons ($\sum\Delta Y_{\text{Cell}}$) produced in a cell should vary around 0. Hence,

$$f(\Delta Y) = \sum\Delta Y_{\text{Cell}} = \sum\Delta Y_{\text{Metab-}} + \sum\Delta Y_{\text{Metab+}} + \sum\Delta Y_{\text{ETC+}} = 0 \qquad (3)$$

By detailing ΔY_{Metab} of equation (3) for proliferating cells with data from Fig. 2, we obtained

$$\begin{aligned} f(\Delta Y) = \\ &(\sum\Delta Y_{\text{Pyr-,Glc}} + \sum\Delta Y_{\text{CO}_2\text{-,Pyr}}/\sum\Delta Y_{\text{Lac+,Pyr}}) + \sum\Delta Y_{\text{CAC-}} + \sum\Delta Y_{\text{ETC+}} \\ &+ (\sum\Delta Y^{oPPP}_{\text{Rib-,Glc}}/\sum\Delta Y^{nPPP}_{\text{Rib 0,Glc}} + \sum\Delta Y_{\text{Nuc-}}) \\ &+ \sum\Delta Y_{\text{Sug-,Glu}}/\sum\Delta Y_{\text{Sug 0,Glc}} \\ &+ (\sum\Delta Y_{\text{Ser-,Glu}}/\sum\Delta Y_{\text{Ser-,Glc}} + \sum\Delta Y_{\text{Ala-,Glu}}/\sum\Delta Y_{\text{Ala 0,Glc}} + \sum\Delta Y_{\text{Asp-,Glu}}/\sum\Delta Y_{\text{Asp 0,Glc}} \\ &\qquad + \sum\Delta Y_{\text{Pro-,Glc}}/\sum\Delta Y_{\text{Pro+,Glu}}) \end{aligned}$$

$$+ (\sum \Delta Y_{\text{Glo-,Glu}} / \sum \Delta Y_{\text{Glo+,Glc}} + \sum \Delta Y_{\text{Cit-,Glc}} / \sum \Delta Y_{\text{Cit 0,Glu}} + \sum \Delta Y_{\text{Palm+,Ac(Glu/Glc)}}$$

$$+ \sum \Delta Y^{Lip}_{\text{Lac+,OAA(Glu/Glc)}} / \sum \Delta Y^{Lip}_{\text{Asp+,OAA(Glu/Glc)}} / \sum \Delta Y^{Lip}_{\text{CAC-,OAA(Glu/Glc)}}) = 0 \quad (4)$$

where $\sum$ means the sum of electrons from all the intracellular reactions, and variables with slashes from different metabolic pathways are optional depending on the availability of nutrients and cellular states. As a cell is a self-organizing system, equation (4) can be flexibly set up to 0. When oxygen is sufficient, the ETC works efficiently. To support ATP generation coupled to the ETC, cells may use the metabolic pathways producing electrons.

Metabolic reprogramming of proliferating cells under hypoxia

Under the condition of ETC dysfunction, such as hypoxia and ETC inhibition, the electron flow to oxygen is blocked ($\Delta Y_{\text{ETC+}} \approx 0$), thus

$$f(\Delta Y) = \sum \Delta Y_{\text{Metab-}} + \sum \Delta Y_{\text{Metab+}} < 0 \quad (5)$$

It could lead to accumulated electrons that unlikely rises infinitely (fig. S4, A-D). Therefore, to equate $f(\Delta Y)$ with 0 while still enable anabolic processes, proliferating cells have to rewire their metabolic reactions to balance electron transfer by reducing the production and enhancing the dissipation of electrons (Fig. 3A). In doing so, $f(\Delta Y)$ is maximized by selecting greater ΔY values from alternative metabolic pathways, thus gives

$$\max f(\Delta Y) =$$

$$
\begin{aligned}
&(\sum\Delta Y_{\text{Pyr-,Glc}} + \sum\Delta Y_{\text{Lac+,Pyr}}) + \sum\Delta Y'_{\text{CAC-}} \\
&+ (\sum\Delta Y^{nPPP}_{\text{Rib 0,Glc}} + \sum\Delta Y_{\text{Nuc-}}) \\
&+ \sum\Delta Y_{\text{Sug 0,Glc}} \\
&+ (\sum\Delta Y_{\text{Ser-,Glc}} + \sum\Delta Y_{\text{Ala 0,Glc}} + \sum\Delta Y_{\text{Asp 0,Glc}} + \sum\Delta Y_{\text{Pro+,Glu}}) \\
&+ (\sum\Delta Y_{\text{Glo+,Glc}} + \sum\Delta Y_{\text{Cit 0,Glu}} + \sum\Delta Y_{\text{Palm+,Ac(Glu)}} + \sum\Delta Y^{Lip}_{\text{Lac+,OAA(Glu)}}/\sum\Delta Y^{Lip}_{\text{Asp+,OAA(Glu)}}) = 0 \qquad (6)
\end{aligned}
$$

In equation (6), glycolytic pyruvate shunts to lactate and avoids entering the CAC to produce electrons (Fig. 2A), which was confirmed by our results that [U-^{13}C]-glucose-derived CAC intermediate, citrate, significantly decreased in human HeLa and mouse 4T1 cells under the condition of hypoxia or ETC inhibition by antimycin A (fig. S5, A-C). Upon anaerobic glycolysis, cells could generate enough ATP by increasing the metabolic flux of glucose to lactate (fig. S5, D-F). This pathway does not release any electron, because $\Delta Y_{\text{Pyr-,Glc}}$ is negatively equal to $\Delta Y_{\text{Lac+,Pyr}}$ (Fig. 2A),

$$\sum\Delta Y^{\text{ATP}}_{\text{Lac,Glc}} = \sum\Delta Y_{\text{Pyr-,Glc}} + \sum\Delta Y_{\text{Lac+,Pyr}} = 0$$

Normally, the CAC produced a great many electrons for mitochondrial ATP generation by completely oxidizing its participants to carbon dioxides, but also provided on purpose some essential intermediates for biosynthesis. Therefore, upon ETC dysfunction, the CAC had to be shaped to a state of low activity required for cell proliferation, endowed with a $\Delta Y'_{\text{CAC-}}$ in equation (6). Our results showed that the metabolic flux of both glucose and glutamine through the CAC was significantly reduced (fig. S5, B and C, and S6, A-C).

As predicted by equation (6), oxidative pentose phosphate pathway (PPP) could be shut down to reduce the production of electrons under hypoxia (*12-14*). Indeed, the fraction of [3-^{2}H]-glucose-derived [^{2}H]-labeled NADPH m+1 via oxidative PPP (*9*) was observed to decline in HeLa cells upon mitochondrial dysfunction (fig. S7, A and B). Therefore, ribose-5-phosphate (R5P) synthesis tends to rely on nonoxidative PPP (*13-15*) with $\Delta Y^{nPPP}_{\mathrm{Rib\ 0,Glc}}$ = 0 (Fig. 2B and fig. S3B). This speculation was verified by measuring ^{13}C enrichment of intracellular sedoheptulose 7-phosphate, a specific intermediate in PPP (Fig. 3B), in HeLa and 4T1 cells supplied with [1,6-$^{13}C_2$]-glucose. [1,6-$^{13}C_2$]-glucose was preferentially processed to sedoheptulose 7-phosphate m+2 in nonoxidative PPP, instead of m+1 via oxidative PPP under hypoxia or upon antimycin A inhibition (Fig. 3C and fig. S7C).

Sugar, serine, alanine and glycerol are directly derived from glucose or glycolytic intermediates, thus their biosynthesis initiated from glucose prevails in proliferating cells (fig. S8, A-F). In contrast, proline is always synthesized from glutamate that is mainly produced from glutamine (fig. S8, G and H). Consistently, these metabolic preferences support equation (6) under hypoxia (Fig. 2, C-E).

Next, we tested the rewiring of glutamine metabolism related to the synthesis of fatty acid and aspartate (Fig. 2, D and E). First, we traced the metabolic pathways by using [U-^{13}C]-glutamine in HeLa cells (Fig. 3D and fig. S5A). Normally, through the CAC, glutamine-derived α-ketoglutarate m+5 was predominantly oxidized to succinate m+4, malate m+4, oxaloacetate m+4 that could be converted into aspartate m+4, citrate m+4 and isocitrate m+4 (Fig. 3, E-G and fig. S6B, D-F). Upon hypoxia or ETC inhibition, glutamine-derived α-ketoglutarate m+5 was reduced by carboxylation to isocitrate m+5 and citrate m+5 that was

further lysed to acetyl-CoA m+2 and oxaloacetate for the generation of aspartate m+3 and malate m+3 (Fig. 3, E-G and fig. S6, D-F). In the meantime, glutamine-derived lactate m+2 from malate m+3 in the reductive pathway dramatically increased while that m+3 from malate m+4 in the oxidative pathway decreased under the condition of hypoxia or ETC inhibition (Fig. 3H). As expected, glutamine-^{13}C was significantly enriched almost in all the measured fatty acids that were synthesized from their precursor, glutamine-derived acetyl-CoA upon ETC dysfunction (Fig. 3I and fig. S9, A-J). These results clearly indicate that cellular metabolism is reprogrammed toward glutamine-initiated lipogenesis through the non-canonical reductive pathway (Fig. 3D), as predicted in equation (6). The similar results were also obtained in 4T1 cells (fig. S6C, G-I), and supported by many recent reports (*16-19*).

Furthermore, simplifying equation (6) by removing all the variables with $\Delta Y = 0$ and rearranging it yielded

$$\max f(\Delta Y) = (\sum \Delta Y'_{\text{CAC-}} + \sum \Delta Y_{\text{Ser-,Glc}} + \sum \Delta Y_{\text{Nuc-}}) + \sum \Delta Y_{\text{Pro+,Glu}} + (\sum \Delta Y_{\text{Glo+,Glc}} + \sum \Delta Y_{\text{Palm+,Ac(Glu)}} + \sum \Delta Y^{Lip}_{\text{Lac+,OAA(Glu)}} / \sum \Delta Y^{Lip}_{\text{Asp+,OAA(Glu)}}) = 0 \quad (7)$$

Electrons were minimally produced by the anabolic transformations including CAC, serine synthesis and nucleic acid synthesis, here designated as $\sum \Delta Y_{-}$. In fact, cells may release additional electrons (section S2.2). Both assimilation of glycerol and metabolism of citrate-derived oxaloacetate are coupled to glutamate-initiated lipid synthesis (Fig. 2E), with the electron production being denoted as $\sum \Delta Y_{\text{Lip+,Glu}}$. Thus, equation (7) is simplified as equation (8),

$$\max f(\Delta Y) = \sum \Delta Y_{-} + \sum \Delta Y_{\mathrm{Pro+,Glu}} + \sum \Delta Y_{\mathrm{Lip+,Glu}} = 0 \quad (8)$$

Obviously, glutamine/glutamate-initiated syntheses of both lipid and proline essentially play a determinative role in metabolically dissipating electrons to support cell proliferation under the condition of ETC dysfunction.

In addition to metabolic rewiring, cells may also survive ETC dysfunction by excreting metabolites that were reduced from the absorbed nutrients, with these metabolic transformations consuming electrons ($\Delta Y > 0$) (Fig. 3J). Based on Y of metabolites listed in Table 1, the conversions of glutamate to proline and pyruvate/oxaloacetate to lactate have positive ΔY values (Fig. 3K). Therefore, the supplement of glutamate, pyruvate (*4-6*) or oxaloacetate (*6*) may facilitate cell survival under the condition of ETC dysfunction (Fig. S10, A-G and section S1.3). Like aspartate (*20*), the concentrations of pyruvate and oxaloacetate in the human blood are very low (*21*), thus they unlikely exert *in vivo* a positive role in removing intracellular electrons in proliferating cells suffering from hypoxia. By contrast, blood glutamate is relatively rich and thus glutamate flux to proline can be potentially employed by cells.

The potential metabolic pathways centered on proline synthesis

Collectively, hypoxia and ETC inhibition rewired metabolic pathways almost in the same fashion according to equation (6), and they also induced similar changes in intracellular metabolites (fig. S11). As revealed in equation (8), cancer cells can accommodate to hypoxia

by initiating glutamine/glutamate-derived lipid and/or proline. Here the overall ΔY value for the equivalent of each glutamine/glutamate-associated metabolic reactions (GMR) is denoted as

$$\Delta Y/\mathrm{GMR} = \Delta Y_{\mathrm{Pro+,Glu}} + \Delta Y_{\mathrm{Lipid+,Glu}}$$

The greater ΔY/GMR value should better benefit cell proliferation under hypoxia. However, inhibition of proline synthesis by depleting the critical enzyme P5CS marginally sensitized cells to hypoxia (fig. S12, A and B). This should be attributable to the fact that cells *in vitro* almost exclusively rely on *de novo* lipogenesis. When proline synthesis was inhibited, the total available glutamate ($\mathrm{Glu_t}$) was primarily diverted to synthesize lipid, palmitate listed here for quantitation, to consume electrons under hypoxia (Fig. 4A). Hence,

$$\Delta Y/\mathrm{GMR} \approx \Delta Y_{\mathrm{Palm+,Glu_t}} = +2.75$$

Nevertheless, the conversion of glutamate to proline has a more efficient ΔY/ATP ratio of +2, compared to the glutamate-initiated palmitate synthesis with a ΔY/ATP of about +1.5 (fig. S13). Therefore, cells may utilize extracellular lipid and shift glutamate from lipid synthesis to secretory proline synthesis in the hypoxic *in vivo* microenvironment, only if they can directly acquire amino acids or obtain nitrogen source for amino acid synthesis (Fig. 4B). When providing nitrogen source, the carbon atoms of alanine, the second most abundant amino acid in human blood, can be converted to excretory lactate, and this process does not

produce electron ($\Delta Y = 0$) (Fig. 4B). As for these transformations,

$$\Delta Y/\mathrm{GMR} = \Delta Y^{\uparrow}_{\mathrm{Pro+,Glu_t}} = +2$$

where $\Delta Y^{\uparrow}_{\mathrm{Pro+,Glu_t}}$ is the ΔY of secretory proline synthesized from the total available glutamate (Fig. 4B).

In addition, cells could synthesize lipid from other carbon sources with positive ΔY/GMR. Since acetyl-CoA is the precursor of fatty acids, ΔY/GMR depends on the synthesis of acetyl-CoA from other nutrients. Hence,

$$\Delta Y/\mathrm{GMR} = \Delta Y^{\uparrow}_{\mathrm{Pro+,Glu_t}} + \Delta Y_{\mathrm{Palm+,Ac}} + \Delta Y_{\mathrm{Ac,Nutr}} = +3.75 + \Delta Y_{\mathrm{Ac,Nutr}}$$

Some nutrients have a positive ΔY/GMR (table S4). In particular, ΔY/GMR of acetate (+3.75) and leucine (+2.75) (fig. S12, C and D and table S4) is greater than that of glutamine/glutamate (+2 ~ +2.75) (Fig. 4, A and B), thus they could be preferentially utilized for lipogensis under hypoxia (*22-26*). These metabolic pathways could be cell type-specific and context-dependent, but all of them are centered on proline synthesis. Therefore, proline synthesis may play a critical role in supporting *in vivo* growth of cancers, which recently were reported in some cancers (*27-29*).

The potential treatments for cancers

Based on all the above analyses, the simultaneous blockage of both proline and lipid syntheses should effectively disable *in vivo* growth of cancers due to their hypoxic

micro-environment. The involved critical enzymes could be the potential targets, including P5CS and P5CR1/2 (*27*) in proline biosynthesis pathway, ACSS1/2 (*24*, *26*), ACL (*30*) and BCAT1/2 (*31*) in the biosynthesis of acetyl-CoA from acetate, citrate and leucine, ACC1/2 (*32*) and HMGR (*33*), the rate-limiting enzymes in the biosynthesis of lipids, mainly fatty acids and sterols (Fig. 4C). Since acetyl-CoA is also required for acetylation of many proteins, serious blockage of the production of acetyl-CoA might be toxic to normal cells. Therefore, blocking acetyl-CoA assimilation by targeting ACC1/2 and HMGR could be the preferential strategy to inhibit lipid synthesis. Since no inhibitor against proline synthesis is available, we used P5CS-null and -wild type 4T1 cells to generate mouse tumor model. When compared to P5CS-expressing cells, P5CS-null cells expanded similarly *in vivo* but more sensitive to PF-05175157 (*34*) and/or lovastatin (*35*), the inhibitors of ACC1/2 and HMGR (Fig. 4D and fig. S14).

Discussion

Due to the fast growth rate and poor vasculature, tumor cells often suffer from insufficient supply with nutrition and oxygen (*3*). To maintain uptake of nutrients, tumor cells usually enhance expression of their transporters (*36*-*38*). However, oxygen passively diffuses into cells, and thus tumor cells are unable to acquire enough oxygen under hypoxia. Instead, they adapt to such harsh conditions by genetically or epigenetically optimizing their metabolism according to max$f(\Delta Y)$, as revealed in the current study. Therefore, cancer cells still display some hypoxia-associated metabolic phenomena even if they are *in vitro* cultured. This essentially interprets metabolic phenomena in cancers (*1*, *2*, *39*), such as abnormal glucose

metabolism (*40*), ectopic utilization of alanine (*41*) and branched-chained amino acid (*31, 42*), active proline synthesis (*27, 28*), and *de novo* lipid synthesis from glutamine (*16-18*) or acetate (*22-24, 26, 43, 44*).

Lipid synthesis occurs in the cytosol and expends NADPH. However, nonoxidative PPP without NADPH generation is preferentially used in cancer cells (*12-15, 44*) to avoid producing electrons. Therefore, some substitutive metabolic reactions, such as oxidation of malate to pyruvate (*45, 46*), conversion of isocitrate to α-ketoglutarate (*16, 17*), and serine/one carbon metabolism (*9, 47, 48*), could be the major source of cellular NADPH. The continuous supplement of NADPH by these reactions relies on metabolic shuttles between the cytosol and mitochondria (*9, 16, 45*). These shuttles essentially convert mitochondrial NADPH/NADH to cytosolic NADPH (section S2.3).

Metabolic reprogramming can be promoted by numerous signal transduction pathways with a high degree of heterogeneity in cancer cells (*1-3*). Importantly, bypassing these intricate and interchangeable cascades, now we can readily control electron transfer under hypoxia by inhibiting the synthesis of both proline and lipid through a cocktail of treatments. Moreover, these inhibitors are expected to be nontoxic to normal cells that can survive on blood lipid and proline supply. Therefore, they appear to be a promising broad-spectrum treatment for solid tumors, and may be more effective if in combination with angiogenic inhibitors that block formation of new blood vessels in tumors or with biguanides that impair the ETC to exacerbate hypoxia.

References

1. L. K. Boroughs, R. J. DeBerardinis, Metabolic pathways promoting cancer cell survival and growth. *Nat Cell Biol* **17**, 351-359 (2015); published online EpubApr (10.1038/ncb3124).

2. N. N. Pavlova, C. B. Thompson, The Emerging Hallmarks of Cancer Metabolism. *Cell Metab* **23**, 27-47 (2016); published online EpubJan 12 (10.1016/j.cmet.2015.12.006).

3. U. E. Martinez-Outschoorn, M. Peiris-Pages, R. G. Pestell, F. Sotgia, M. P. Lisanti, Cancer metabolism: a therapeutic perspective. *Nat Rev Clin Oncol*, (2016); published online EpubMay 04 (10.1038/nrclinonc.2016.60).

4. L. B. Sullivan, D. Y. Gui, A. M. Hosios, L. N. Bush, E. Freinkman, M. G. Vander Heiden, Supporting Aspartate Biosynthesis Is an Essential Function of Respiration in Proliferating Cells. *Cell* **162**, 552-563 (2015); published online EpubJul 30 (10.1016/j.cell.2015.07.017).

5. K. Birsoy, T. Wang, W. W. Chen, E. Freinkman, M. Abu-Remaileh, D. M. Sabatini, An Essential Role of the Mitochondrial Electron Transport Chain in Cell Proliferation Is to Enable Aspartate Synthesis. *Cell* **162**, 540-551 (2015); published online EpubJul 30 (10.1016/j.cell.2015.07.016).

6. D. V. Titov, V. Cracan, R. P. Goodman, J. Peng, Z. Grabarek, V. K. Mootha, Complementation of mitochondrial electron transport chain by manipulation of the NAD+/NADH ratio. *Science* **352**, 231-235 (2016); published online EpubApr 8 (10.1126/science.aad4017).

7. S. Harayama, M. Kok, E. L. Neidle, Functional and evolutionary relationships among diverse oxygenases. *Annu Rev Microbiol* **46**, 565-601 (1992)10.1146/annurev.mi.46.100192.003025).

8. W. D. Lienhart, V. Gudipati, P. Macheroux, The human flavoproteome. *Arch Biochem Biophys* **535**, 150-162 (2013); published online EpubJul 15 (10.1016/j.abb.2013.02.015).

9. C. A. Lewis, S. J. Parker, B. P. Fiske, D. McCloskey, D. Y. Gui, C. R. Green, N. I. Vokes, A. M. Feist, M. G. Vander Heiden, C. M. Metallo, Tracing compartmentalized NADPH metabolism in

the cytosol and mitochondria of mammalian cells. *Mol Cell* **55**, 253-263 (2014); published online EpubJul 17 (10.1016/j.molcel.2014.05.008).

10. B. Alberts, J. H. Wilson, T. Hunt, *Molecular biology of the cell*. (Garland Science, New York, ed. 5th, 2008), pp. xxxiii, 1601, 1690 p.

11. J. L. Coloff, J. P. Murphy, C. R. Braun, I. S. Harris, L. M. Shelton, K. Kami, S. P. Gygi, L. M. Selfors, J. S. Brugge, Differential Glutamate Metabolism in Proliferating and Quiescent Mammary Epithelial Cells. *Cell Metab* **23**, 867-880 (2016); published online EpubMay 10 (10.1016/j.cmet.2016.03.016).

12. D. Samanta, Y. Park, S. A. Andrabi, L. M. Shelton, D. M. Gilkes, G. L. Semenza, PHGDH Expression Is Required for Mitochondrial Redox Homeostasis, Breast Cancer Stem Cell Maintenance, and Lung Metastasis. *Cancer Res* **76**, 4430-4442 (2016); published online EpubAug 01 (10.1158/0008-5472.CAN-16-0530).

13. H. Ying, A. C. Kimmelman, C. A. Lyssiotis, S. Hua, G. C. Chu, E. Fletcher-Sananikone, J. W. Locasale, J. Son, H. Zhang, J. L. Coloff, H. Yan, W. Wang, S. Chen, A. Viale, H. Zheng, J. H. Paik, C. Lim, A. R. Guimaraes, E. S. Martin, J. Chang, A. F. Hezel, S. R. Perry, J. Hu, B. Gan, Y. Xiao, J. M. Asara, R. Weissleder, Y. A. Wang, L. Chin, L. C. Cantley, R. A. DePinho, Oncogenic Kras maintains pancreatic tumors through regulation of anabolic glucose metabolism. *Cell* **149**, 656-670 (2012); published online EpubApr 27 (10.1016/j.cell.2012.01.058).

14. S. K. Shukla, V. Purohit, K. Mehla, V. Gunda, N. V. Chaika, E. Vernucci, R. J. King, J. Abrego, G. D. Goode, A. Dasgupta, A. L. Illies, T. Gebregiworgis, B. Dai, J. J. Augustine, D. Murthy, K. S. Attri, O. Mashadova, P. M. Grandgenett, R. Powers, Q. P. Ly, A. J. Lazenby, J. L. Grem, F. Yu, J. M. Mates, J. M. Asara, J. W. Kim, J. H. Hankins, C. Weekes, M. A. Hollingsworth, N. J. Serkova,

A. R. Sasson, J. B. Fleming, J. M. Oliveto, C. A. Lyssiotis, L. C. Cantley, L. Berim, P. K. Singh, MUC1 and HIF-1alpha Signaling Crosstalk Induces Anabolic Glucose Metabolism to Impart Gemcitabine Resistance to Pancreatic Cancer. *Cancer Cell* **32**, 71-87 e77 (2017); published online EpubJul 10 (10.1016/j.ccell.2017.06.004).

15. L. G. Boros, J. S. Torday, S. Lim, S. Bassilian, M. Cascante, W. N. Lee, Transforming growth factor beta2 promotes glucose carbon incorporation into nucleic acid ribose through the nonoxidative pentose cycle in lung epithelial carcinoma cells. *Cancer Res* **60**, 1183-1185 (2000); published online EpubMar 01 (

16. A. R. Mullen, W. W. Wheaton, E. S. Jin, P. H. Chen, L. B. Sullivan, T. Cheng, Y. Yang, W. M. Linehan, N. S. Chandel, R. J. DeBerardinis, Reductive carboxylation supports growth in tumour cells with defective mitochondria. *Nature* **481**, 385-388 (2011); published online EpubNov 20 (10.1038/nature10642).

17. C. M. Metallo, P. A. Gameiro, E. L. Bell, K. R. Mattaini, J. Yang, K. Hiller, C. M. Jewell, Z. R. Johnson, D. J. Irvine, L. Guarente, J. K. Kelleher, M. G. Vander Heiden, O. Iliopoulos, G. Stephanopoulos, Reductive glutamine metabolism by IDH1 mediates lipogenesis under hypoxia. *Nature* **481**, 380-384 (2011); published online EpubNov 20 (10.1038/nature10602).

18. D. R. Wise, P. S. Ward, J. E. Shay, J. R. Cross, J. J. Gruber, U. M. Sachdeva, J. M. Platt, R. G. DeMatteo, M. C. Simon, C. B. Thompson, Hypoxia promotes isocitrate dehydrogenase-dependent carboxylation of alpha-ketoglutarate to citrate to support cell growth and viability. *Proc Natl Acad Sci U S A* **108**, 19611-19616 (2011); published online EpubDec 6 (10.1073/pnas.1117773108).

19. A. R. Mullen, Z. Hu, X. Shi, L. Jiang, L. K. Boroughs, Z. Kovacs, R. Boriack, D. Rakheja, L. B. Sullivan, W. M. Linehan, N. S. Chandel, R. J. DeBerardinis, Oxidation of alpha-ketoglutarate is

required for reductive carboxylation in cancer cells with mitochondrial defects. *Cell Rep* **7**, 1679-1690 (2014); published online EpubJun 12 (10.1016/j.celrep.2014.04.037).

20. J. A. Wuu, L. Y. Wen, T. Y. Chuang, G. G. Chang, Amino acid concentrations in serum and aqueous humor from subjects with extreme myopia or senile cataract. *Clin Chem* **34**, 1610-1613 (1988); published online EpubAug (

21. H. A. Krebs, Chemical composition of blood plasma and serum. *Annu Rev Biochem* **19**, 409-430 (1950)10.1146/annurev.bi.19.070150.002205).

22. S. A. Comerford, Z. Huang, X. Du, Y. Wang, L. Cai, A. K. Witkiewicz, H. Walters, M. N. Tantawy, A. Fu, H. C. Manning, J. D. Horton, R. E. Hammer, S. L. McKnight, B. P. Tu, Acetate dependence of tumors. *Cell* **159**, 1591-1602 (2014); published online EpubDec 18 (10.1016/j.cell.2014.11.020).

23. Z. T. Schug, J. Vande Voorde, E. Gottlieb, The metabolic fate of acetate in cancer. *Nat Rev Cancer* **16**, 708-717 (2016); published online EpubNov (10.1038/nrc.2016.87).

24. Z. T. Schug, B. Peck, D. T. Jones, Q. Zhang, S. Grosskurth, I. S. Alam, L. M. Goodwin, E. Smethurst, S. Mason, K. Blyth, L. McGarry, D. James, E. Shanks, G. Kalna, R. E. Saunders, M. Jiang, M. Howell, F. Lassailly, M. Z. Thin, B. Spencer-Dene, G. Stamp, N. J. van den Broek, G. Mackay, V. Bulusu, J. J. Kamphorst, S. Tardito, D. Strachan, A. L. Harris, E. O. Aboagye, S. E. Critchlow, M. J. Wakelam, A. Schulze, E. Gottlieb, Acetyl-CoA synthetase 2 promotes acetate utilization and maintains cancer cell growth under metabolic stress. *Cancer Cell* **27**, 57-71 (2015); published online EpubJan 12 (10.1016/j.ccell.2014.12.002).

25. S. B. Crown, N. Marze, M. R. Antoniewicz, Catabolism of Branched Chain Amino Acids Contributes Significantly to Synthesis of Odd-Chain and Even-Chain Fatty Acids in 3T3-L1

Adipocytes. *PLoS One* **10**, e0145850 (2015)10.1371/journal.pone.0145850).

26. X. Gao, S. H. Lin, F. Ren, J. T. Li, J. J. Chen, C. B. Yao, H. B. Yang, S. X. Jiang, G. Q. Yan, D. Wang, Y. Wang, Y. Liu, Z. Cai, Y. Y. Xu, J. Chen, W. Yu, P. Y. Yang, Q. Y. Lei, Acetate functions as an epigenetic metabolite to promote lipid synthesis under hypoxia. *Nat Commun* **7**, 11960 (2016); published online EpubJun 30 (10.1038/ncomms11960).

27. F. Loayza-Puch, K. Rooijers, L. C. Buil, J. Zijlstra, J. F. Oude Vrielink, R. Lopes, A. P. Ugalde, P. van Breugel, I. Hofland, J. Wesseling, O. van Tellingen, A. Bex, R. Agami, Tumour-specific proline vulnerability uncovered by differential ribosome codon reading. *Nature* **530**, 490-494 (2016); published online EpubFeb 25 (10.1038/nature16982).

28. W. Liu, A. Le, C. Hancock, A. N. Lane, C. V. Dang, T. W. Fan, J. M. Phang, Reprogramming of proline and glutamine metabolism contributes to the proliferative and metabolic responses regulated by oncogenic transcription factor c-MYC. *Proc Natl Acad Sci U S A* **109**, 8983-8988 (2012); published online EpubJun 5 (10.1073/pnas.1203244109).

29. J. M. Phang, W. Liu, C. Hancock, K. J. Christian, The proline regulatory axis and cancer. *Front Oncol* **2**, 60 (2012)10.3389/fonc.2012.00060).

30. G. Hatzivassiliou, F. Zhao, D. E. Bauer, C. Andreadis, A. N. Shaw, D. Dhanak, S. R. Hingorani, D. A. Tuveson, C. B. Thompson, ATP citrate lyase inhibition can suppress tumor cell growth. *Cancer Cell* **8**, 311-321 (2005); published online EpubOct (10.1016/j.ccr.2005.09.008).

31. M. Tonjes, S. Barbus, Y. J. Park, W. Wang, M. Schlotter, A. M. Lindroth, S. V. Pleier, A. H. Bai, D. Karra, R. M. Piro, J. Felsberg, A. Addington, D. Lemke, I. Weibrecht, V. Hovestadt, C. G. Rolli, B. Campos, S. Turcan, D. Sturm, H. Witt, T. A. Chan, C. Herold-Mende, R. Kemkemer, R. Konig, K. Schmidt, W. E. Hull, S. M. Pfister, M. Jugold, S. M. Hutson, C. Plass, J. G. Okun, G.

Reifenberger, P. Lichter, B. Radlwimmer, BCAT1 promotes cell proliferation through amino acid catabolism in gliomas carrying wild-type IDH1. *Nat Med* **19**, 901-908 (2013); published online EpubJul (10.1038/nm.3217).

32. R. U. Svensson, S. J. Parker, L. J. Eichner, M. J. Kolar, M. Wallace, S. N. Brun, P. S. Lombardo, J. L. Van Nostrand, A. Hutchins, L. Vera, L. Gerken, J. Greenwood, S. Bhat, G. Harriman, W. F. Westlin, H. J. Harwood, Jr., A. Saghatelian, R. Kapeller, C. M. Metallo, R. J. Shaw, Inhibition of acetyl-CoA carboxylase suppresses fatty acid synthesis and tumor growth of non-small-cell lung cancer in preclinical models. *Nat Med* **22**, 1108-1119 (2016); published online EpubOct (10.1038/nm.4181).

33. J. E. Stine, H. Guo, X. Sheng, X. Han, M. N. Schointuch, T. P. Gilliam, P. A. Gehrig, C. Zhou, V. L. Bae-Jump, The HMG-CoA reductase inhibitor, simvastatin, exhibits anti-metastatic and anti-tumorigenic effects in ovarian cancer. *Oncotarget* **7**, 946-960 (2016); published online EpubJan 5 (10.18632/oncotarget.5834).

34. D. A. Griffith, D. W. Kung, W. P. Esler, P. A. Amor, S. W. Bagley, C. Beysen, S. Carvajal-Gonzalez, S. D. Doran, C. Limberakis, A. M. Mathiowetz, K. McPherson, D. A. Price, E. Ravussin, G. E. Sonnenberg, J. A. Southers, L. J. Sweet, S. M. Turner, F. F. Vajdos, Decreasing the rate of metabolic ketone reduction in the discovery of a clinical acetyl-CoA carboxylase inhibitor for the treatment of diabetes. *J Med Chem* **57**, 10512-10526 (2014); published online EpubDec 26 (10.1021/jm5016022).

35. J. A. Tobert, Lovastatin and beyond: the history of the HMG-CoA reductase inhibitors. *Nat Rev Drug Discov* **2**, 517-526 (2003); published online EpubJul (10.1038/nrd1112).

36. J. S. Flier, M. M. Mueckler, P. Usher, H. F. Lodish, Elevated levels of glucose transport and

transporter messenger RNA are induced by ras or src oncogenes. *Science* **235**, 1492-1495 (1987); published online EpubMar 20 (

37. D. R. Wise, R. J. DeBerardinis, A. Mancuso, N. Sayed, X. Y. Zhang, H. K. Pfeiffer, I. Nissim, E. Daikhin, M. Yudkoff, S. B. McMahon, C. B. Thompson, Myc regulates a transcriptional program that stimulates mitochondrial glutaminolysis and leads to glutamine addiction. *Proc Natl Acad Sci U S A* **105**, 18782-18787 (2008); published online EpubDec 2 (10.1073/pnas.0810199105).
38. D. R. Wise, C. B. Thompson, Glutamine addiction: a new therapeutic target in cancer. *Trends Biochem Sci* **35**, 427-433 (2010); published online EpubAug (10.1016/j.tibs.2010.05.003).
39. A. Vazquez, J. J. Kamphorst, E. K. Markert, Z. T. Schug, S. Tardito, E. Gottlieb, Cancer metabolism at a glance. *J Cell Sci* **129**, 3367-3373 (2016); published online EpubSep 15 (10.1242/jcs.181016).
40. O. Warburg, On the origin of cancer cells. *Science* **123**, 309-314 (1956); published online EpubFeb 24 (
41. C. M. Sousa, D. E. Biancur, X. Wang, C. J. Halbrook, M. H. Sherman, L. Zhang, D. Kremer, R. F. Hwang, A. K. Witkiewicz, H. Ying, J. M. Asara, R. M. Evans, L. C. Cantley, C. A. Lyssiotis, A. C. Kimmelman, Pancreatic stellate cells support tumour metabolism through autophagic alanine secretion. *Nature* **536**, 479-483 (2016); published online EpubAug 25 (10.1038/nature19084).
42. J. R. Mayers, C. Wu, C. B. Clish, P. Kraft, M. E. Torrence, B. P. Fiske, C. Yuan, Y. Bao, M. K. Townsend, S. S. Tworoger, S. M. Davidson, T. Papagiannakopoulos, A. Yang, T. L. Dayton, S. Ogino, M. J. Stampfer, E. L. Giovannucci, Z. R. Qian, D. A. Rubinson, J. Ma, H. D. Sesso, J. M. Gaziano, B. B. Cochrane, S. Liu, J. Wactawski-Wende, J. E. Manson, M. N. Pollak, A. C. Kimmelman, A. Souza, K. Pierce, T. J. Wang, R. E. Gerszten, C. S. Fuchs, M. G. Vander Heiden,

B. M. Wolpin, Elevation of circulating branched-chain amino acids is an early event in human pancreatic adenocarcinoma development. *Nat Med* **20**, 1193-1198 (2014); published online EpubOct (10.1038/nm.3686).

43. J. J. Kamphorst, M. K. Chung, J. Fan, J. D. Rabinowitz, Quantitative analysis of acetyl-CoA production in hypoxic cancer cells reveals substantial contribution from acetate. *Cancer Metab* **2**, 23 (2014)10.1186/2049-3002-2-23).

44. M. G. Vander Heiden, R. J. DeBerardinis, Understanding the Intersections between Metabolism and Cancer Biology. *Cell* **168**, 657-669 (2017); published online EpubFeb 9 (10.1016/j.cell.2016.12.039).

45. P. Jiang, W. Du, A. Mancuso, K. E. Wellen, X. Yang, Reciprocal regulation of p53 and malic enzymes modulates metabolism and senescence. *Nature* **493**, 689-693 (2013); published online EpubJan 31 (10.1038/nature11776).

46. J. Son, C. A. Lyssiotis, H. Ying, X. Wang, S. Hua, M. Ligorio, R. M. Perera, C. R. Ferrone, E. Mullarky, N. Shyh-Chang, Y. Kang, J. B. Fleming, N. Bardeesy, J. M. Asara, M. C. Haigis, R. A. DePinho, L. C. Cantley, A. C. Kimmelman, Glutamine supports pancreatic cancer growth through a KRAS-regulated metabolic pathway. *Nature* **496**, 101-105 (2013); published online EpubApr 4 (10.1038/nature12040).

47. J. Fan, J. Ye, J. J. Kamphorst, T. Shlomi, C. B. Thompson, J. D. Rabinowitz, Quantitative flux analysis reveals folate-dependent NADPH production. *Nature* **510**, 298-302 (2014); published online EpubJun 12 (10.1038/nature13236).

48. J. Ye, J. Fan, S. Venneti, Y. W. Wan, B. R. Pawel, J. Zhang, L. W. Finley, C. Lu, T. Lindsten, J. R. Cross, G. Qing, Z. Liu, M. C. Simon, J. D. Rabinowitz, C. B. Thompson, Serine catabolism

regulates mitochondrial redox control during hypoxia. *Cancer Discov* **4**, 1406-1417 (2014); published online EpubDec (10.1158/2159-8290.CD-14-0250).

ACKNOWLEDGEMENTS

We thank Dr. Ceshi Chen (Kunming Institute of Zoology, Chinese Academy of Sciences) and Dr. Qunying Lei (Fudan University, China) for carefully reading through the manuscript and valuable discussion and also thank Dr. Xiaohui Liu (Metabolomics Facility at Tsinghua University Branch of China National Center for Protein Sciences, China) for technical help. This work is supported by Grants 81622037, 81372185 and 81672762 from Natural Science Foundation of China. B.L. conceived and designed the study, and developed the model and derived the equations; Y.W. and M.L. performed experiments; Y.W., M.L. and B.L. analyzed the data; Y.R., Q.C. and Y.C. created some constructs and cell lines; G.Y. provided constructive advice and in particular coined the term of "*free electron potential*" whose symbol, "*Y*", is the first letter of his last name; B.L. wrote the paper.

Figures

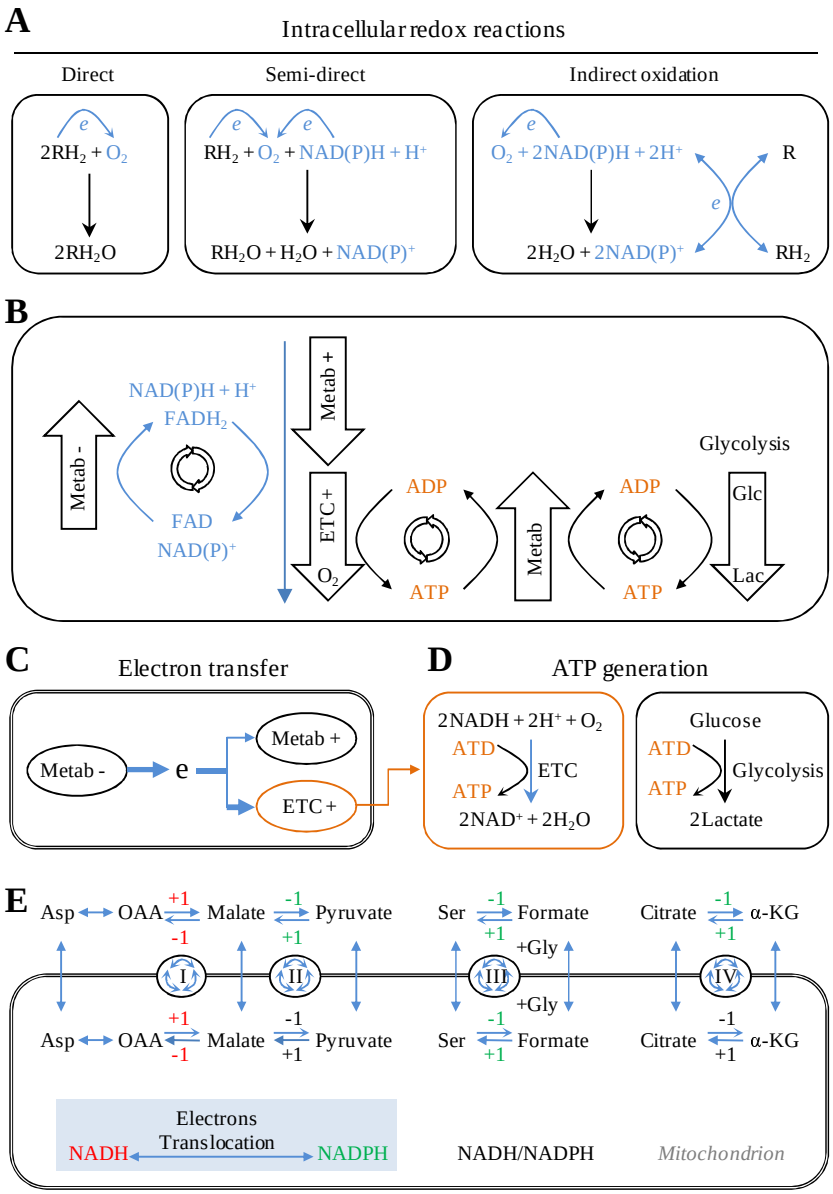

Figure 1. Electron transfer in intracellular metabolism. (A) Intracellular redox reactions including direct, semi-direct and indrect oxidations. (B) Intracellular electron transfer. Metab-, the electrons-releasing metabolic transformations; metab+, the electrons-consuming metabolic transformations; ETC+, the mitochondrial electron transport chain that consumes electrons. (C) A model for electron transfer in cells. (D) Intracellular ATP generation. ATP can

be generated in mitochondria that is coupled to electros consumption in ETC, or be produced in the glycolytic pathway that is independent of electron transfer. (E) Translocation of electrons (fig S1). Electrons in NADH + H^+ or NADPH + H^+ can be translocated spatially or to each other. "-", the production of electrons; "+", the dissipation of electrons; Red number, NADH + H^+; Green number, NADPH + H^+; Black number, NADH + H^+ or NADPH + H^+.

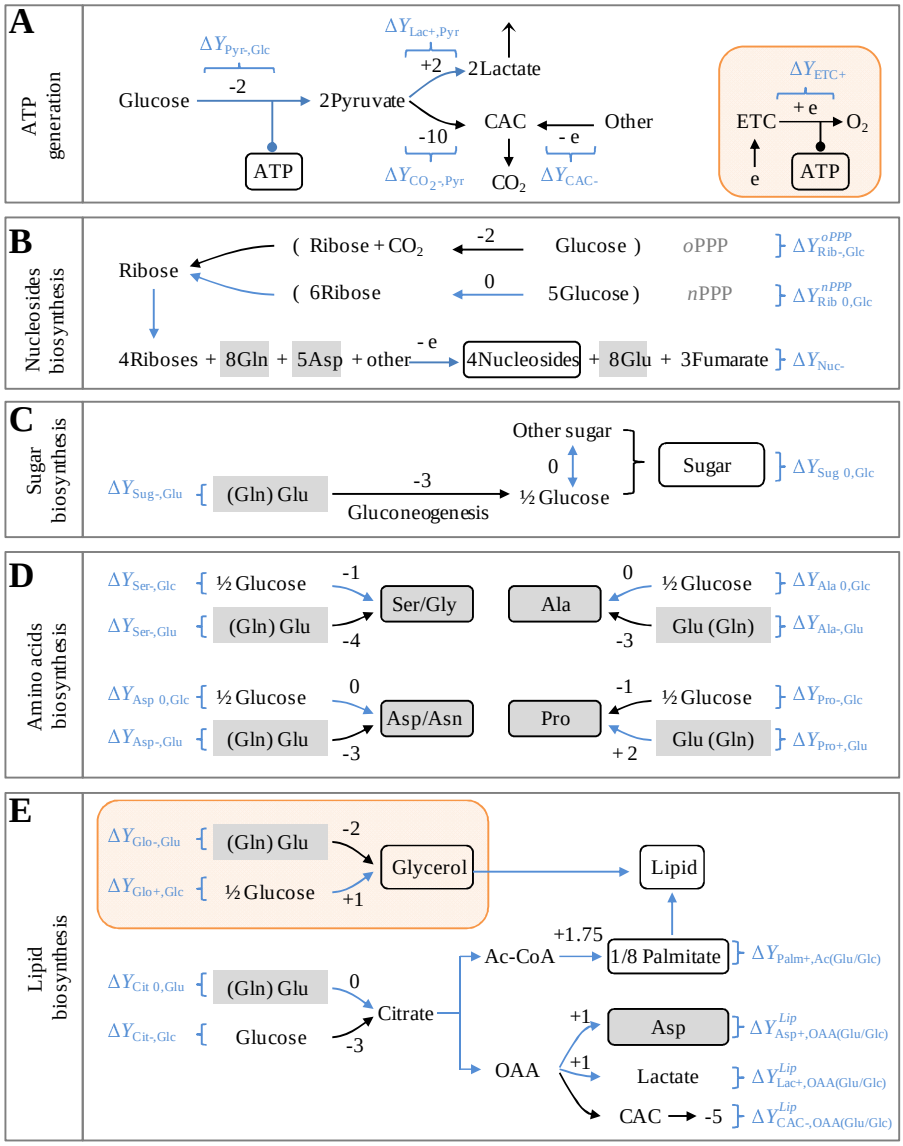

Figure 2. The production or dissipation of electrons (Δ*Y*) in metabolic transformations. Δ*Y* is calculated by equation (2) based on *Y* values in Table 1 and table S1. (A) Δ*Y* in ATP generation. The inset is mitochondrial ATP generation. (B) Δ*Y* in the biosynthesis of nucleosides. Ribose can be generated in oxidative PPP (*o*PPP) or non-oxidative PPP (*n*PPP). The exact Δ*Y* values of ribose-initiated biosynthesis of nucleosides depend on the specified nucleoside. See Extended Data Fig. 2 and Tabel3 for details. (C) Δ*Y* in the biosynthesis of

sugar. (D) ΔY in the biosynthesis of non-essential amino acids. The carbons of amino acids could be from glucose or glutamine. (E) ΔY in the biosynthesis of lipids. Palmitate could be synthesized from glucose or glutamine. The inset is the biosynthesis of glycerol (glycerol-3-phosphate). In all panels, numbers are ΔY values in one reaction. "-" means the prodution of electrons while "+" refers to the consumption of electrons. ▢ indicates the building bricks for proliferating cells. ▭ shows amino acids. Curve arrow indicates optional pathways. ⊣⊏ represents the coupled pathwys. Blue routes show the metabolic pathways prevailing under hypoxia.

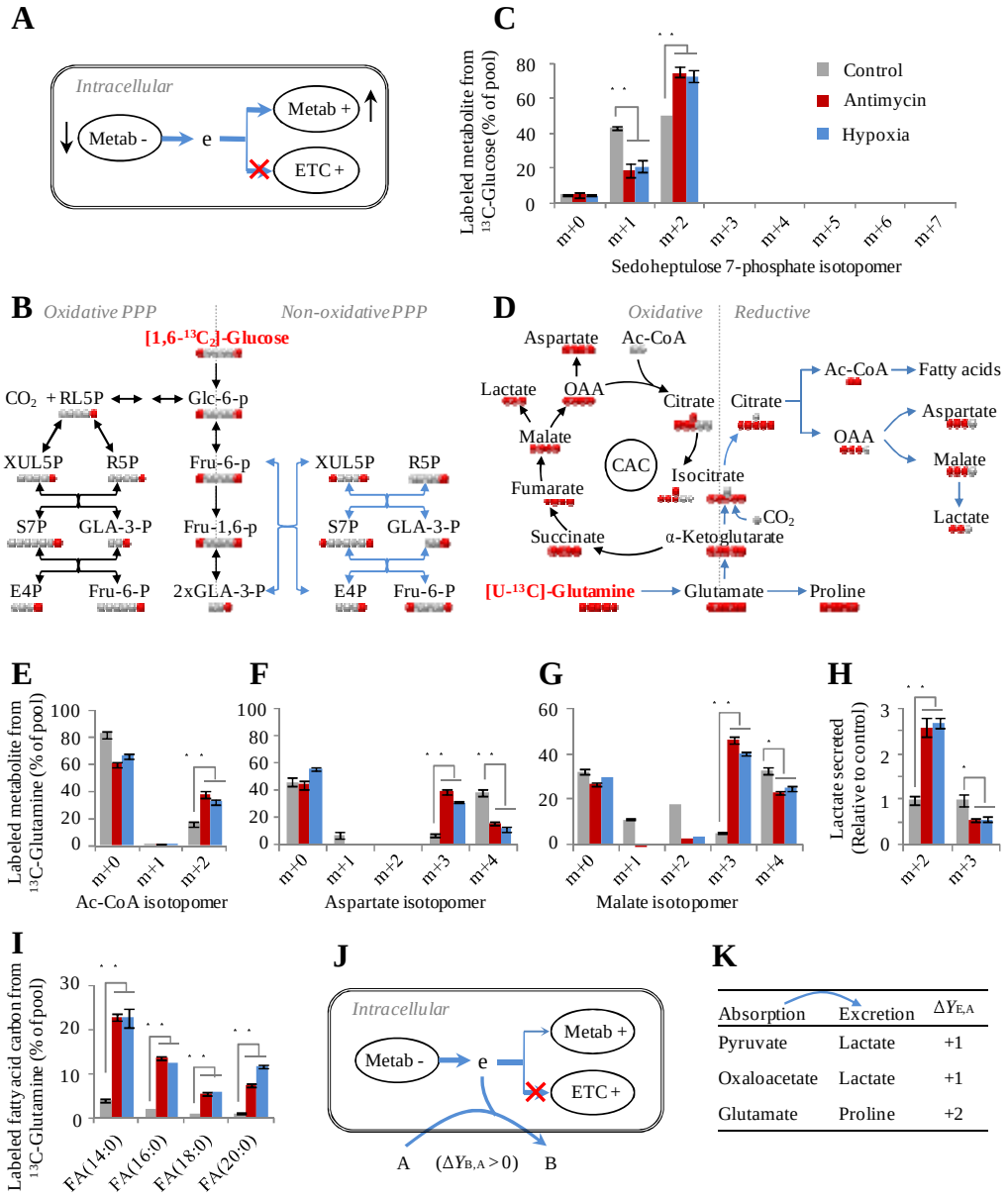

Figure 3. Metabolic reprogramming in proliferating cells with ETC dysfunction. (A) A model to show that cells adapt to ETC dysfunction by optimizing their metabolic pathways: using electrons-consuming and avoiding electrons-producing pathways. (B) Schematics for oxidative pentose phosphate pathway (*o*PPP) and non-oxidative pentose phosphate pathway (*n*PPP). (C) Mass isotopomer analysis of sedoheptulose-7-phosphate in HeLa cells cultured with D-[1,6-$^{13}C_2$]-glucose for 8h under the conditions of hypoxia or inhibition by antimycin A

(1 μM). (D) Schematic of oxidative or reductive glutamine metabolism. (E-G) Mass isotopomer analysis of acetyl-CoA, aspartate and malate in HeLa cells cultured with $^{13}C_5$-glutamine for 8h under the conditions of hypoxia or inhibition by antimycin A (1 μM). (H) Secretion of lactate from HeLa cells under the same condition as described in (E-G). (I) Labeled carbons in fatty acids in HeLa cells cultured with $^{13}C_5$-glutamine for 48h under the conditions of hypoxia or inhibition by antimycin A (1 μM). (J) A model to show that cells adapt to ETC dysfunction by metabolically excreting electrons. (K) Potential excretory metabolites with electrons consumption. Data are the mean ± SD for three independent cultures. *P<0.05; **P<0.01, Student's t-test.

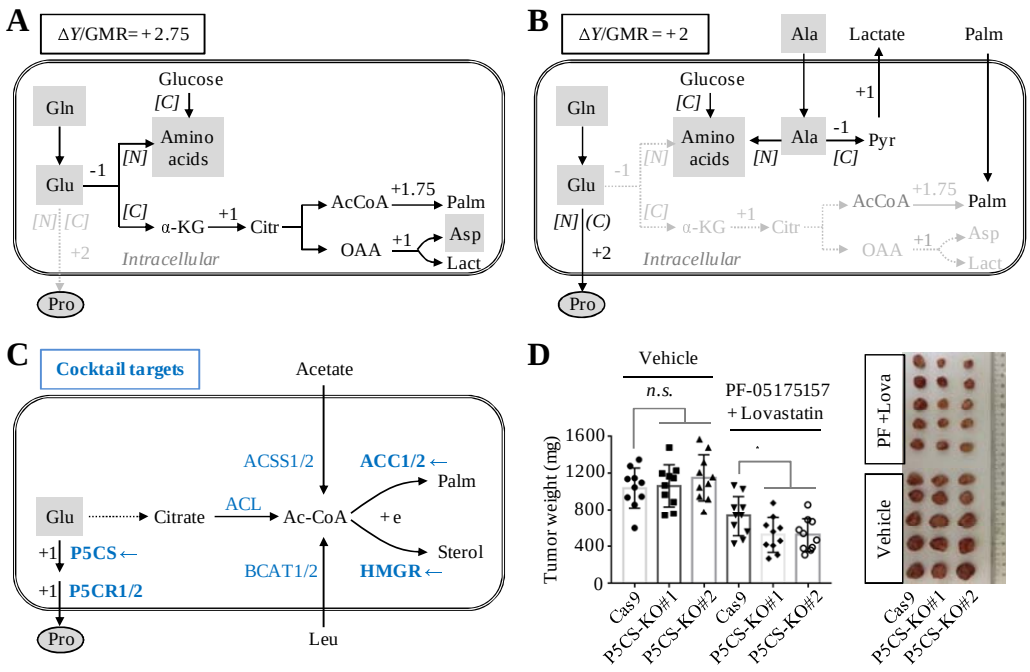

Figure 4. Potential proline synthesis-dependent metabolic adaption in proliferating cells with ETC dysfunction. ΔY/GMR referred to the overall ΔY value for the equivalent of each glutamate-associated metabolic reactions. (A) A model to show the glutamate-initiated palmitate biosynthesis. (B) A model to show glutamate-derived secretory proline. Cells use exogenous lipids/palmitates, and glutamate is used to synthesize proline that is secreted out of cells. Amino acids are absorbed or synthesized from alanine amino group. (C) Potential targets to block electrons-consuming metabolic pathways. (D) Simultaneous inhibition of P5CS, ACC1/2 and HMGR synergistically suppress tumor growth *in vivo*. P5CS, pyrroline-5-carboxylate synthase, is the key enzyme in the synthesis of proline, and it is knockouted in 4T1 cells. PF-05175157 and lovastatin are the inhibitors of ACC1/2, acetyl-CoA carboxylase, and HMGR, 3-hydroxy-3-methyl-glutaryl-coenzyme A reductase.

Table 1. Free electron potential of metabolites

	Metabolites	**Formula**	***Y*,**	**(*Y*/C)***
Carbohydrate	Glucose	$C_6H_{12}O_6$	12	(2.00/C)
	Fructose	$C_6H_{12}O_6$	12	(2.00/C)
	Glyceraldehyde	$C_3H_6O_3$	6	(2.00/C)
	Glyceric acid	$C_3H_6O_4$	5	(1.67/C)
	Pyruvate	$C_3H_4O_3$	5	(1.67/C)
	Lactate	$C_3H_6O_3$	6	(2.00/C)
	Oxaloacetate	$C_4H_4O_5$	5	(1.25/C)
	Malate	$C_4H_6O_5$	6	(1.50/C)
	Fumarate	$C_4H_4O_4$	6	(1.50/C)
	Succinate	$C_4H_6O_4$	7	(1.75/C)
	α-Ketoglutarate	$C_5H_6O_5$	8	(1.60/C)
	Citrate	$C_6H_8O_7$	9	(1.50/C)
Non-essential amino acids	Glycine	$C_2H_5NO_2$	3	(1.50/C)
	Serine	$C_3H_7NO_3$	5	(1.67/C)
	Aspartate	$C_4H_7NO_4$	6	(1.50/C)
	Asparagine	$C_4H_8N_2O_3$	6	(1.50/C)
	Glutamine	$C_5H_{10}N_2O_3$	9	(1.80/C)
	Glutamate	$C_5H_9NO_4$	9	(1.80/C)
	Alanine	$C_3H_7NO_2$	6	(2.00/C)
	Proline	$C_5H_9NO_2$	11	(2.20/C)
Acetyl-CoA	Acetate	$C_2H_4O_2$	4	(2.00/C)
Lipid components	Glycerol	$C_3H_8O_3$	7	(2.33/C)
	Palmitate	$C_{16}H_{32}O_2$	46	(2.875/C)
	Farnesol†	$C_{15}H_{26}O$	42	(2.80/C)

*Y/C is *Y* value per carbon of metabolites.

†Farnesol (farnesyl pyrophosphate) is the precursor of sterols.

Supplementary Mearterials

Supplementary Text

Figs. S1 to S15

Tables S1 to S4

Supplementary Discussion

Materials and Methods

References (49-58)